Environ. Sci. Technol. **1999**, *33,* 1127−1132

Optical Teledetection of Chlorophyll *a* in Turbid Inland Waters

HERMAN J. GONS

Netherlands Institute of Ecology, Centre for Limnology, Rijksstraatweg 6, Nieuwersluis, P.O. Box 1299, 3600 BG Maarssen, The Netherlands

Determination of subsurface spectral irradiance reflectance by use of a hand-held spectroradiometer and then estimation of chlorophyll *a* (Chl-*a*) concentration facilitate assessment of ecological change in turbid lakes, rivers, and estuaries. The method was applied under widely varying solar elevation and weather. Noise due to reflected sky light was evaluated by theory on surface waves and by field data. A strong relationship was established for the shallow and eutrophic freshwater IJssel Lagoon including the River IJssel (The Netherlands) between corrected Chl-*a* concentrations (3−185 mg m^{-3}) and the reflectance ratio for 704 and 672 nm with backscattering derived from the reflectance at 776 nm ($R^2 > 0.95$; $N = 114$; standard error of estimate <9 mg m^{-3}). This relationship adequately predicted Chl-*a* concentrations in well-mixed and optically deep water in lakes in The Netherlands, the Scheldt Estuary in Belgium and The Netherlands, and Lake Tai in China ($N = 40$; standard error of estimate <9 mg m^{-3}). Floating layers of the cyanobacterium *Microcystis* in Lake Chao in China were distinguished from homogeneously distributed phytoplankton by reflectance in the violet, blue, and near-infrared wavebands.

Introduction

Concentration of the photosynthetic pigment chlorophyll *a* [Chl-*a*] is measured as an indicator of water quality and in ecological studies. Distribution of the pigment is pertinent to the impact of climatic change and the scarcity of freshwater resources for economic development. Analysis of a few samples may establish [Chl-*a*] in small, but not in large water bodies (*1*−*3*). As a time saving, cost-effective, and scientifically rewarding alternative, [Chl-*a*] may be equated with spectral reflectance, i.e., intrinsic water color, as determined from water-leaving radiance (*4*−*6*). For marine waters, satisfactory relationships have been described for [Chl-*a*] from 0.02 to 78 mg m^{-3} (*7*). Optical teledetection of Chl-*a* in inland waters appeared to be problematic. Of algorithms for [Chl-*a*] from 0.3 to 350 mg m^{-3} in rivers and lakes (*3, 8*−*12*), up to 480 mg m^{-3} in aquaculture impoundments (*13*), and >2100 mg m^{-3} in mesocosms (*14*) and oxidation ponds (*15*), none has been shown to be accurate beyond particular districts. The slow progress is attributable to optical heterogeneity of inland waters as compared to the oceans. It has long been known that high concentrations of dissolved organic matter [DOM] and total suspended matter [TSM] interfere with optical determination of [Chl-*a*] (*16*). Many inland waters present high [DOM] and highly dynamic detritus and mineral particles of diverse origin, size, and shape (*17*). Prediction of [Chl-*a*] may greatly improve for known spectral absorption and scattering (*18*).

This paper reports on the determination of spectral reflectance immediately below the water surface $R(0,\lambda)$ and then [Chl-*a*] for widely different water quality, solar elevation, and weather. The hand-held apparatus used herein can be instantly deployed, and the computerized scanning and data output allow assessment of [Chl-*a*] in near-real time. On the IJssel Lagoon, including the River IJssel (The Netherlands), optical teledetection was combined with analysis of Chl-*a* (*19, 20*) in near-surface (depth ≤ 0.1 m) and depth-integrated samples. These data served to calibrate [Chl-*a*] retrieval from $R(0,\lambda)$. The method was then validated for small and large, both shallow and relatively deep, lakes and the estuary of a large river.

Study Sites

IJssel Lagoon, August 1993−September 1996. The River IJssel discharges into Lake Ketelmeer (52°35′ N, 5°45′ E; surface area (A) = 35 km^2; mean depth (Z) = 3 m) adjoining Lake IJsselmeer (52°50′ N, 5°20′ E; A = 1190 km^2; Z = 4.5 m). Twelve 60-km-long surveys, under widely different sun angles and skies (Table 1) included the stations River IJssel, central Lake Ketelmeer, and southern (Urk), northwestern (Medemblik) and northeastern Lake IJsselmeer (Stavoren). Water temperatures varied from 6 to 25 °C. Two surveys were made in the rain. Extremely extensive resuspension of sediment occurred at Beaufort-8 wind in March 1994. $R(0,\lambda)$ was not acquired for only one station (Medemblik, March 1994). $R(0,\lambda)$, [Chl-*a*], and [TSM] were also determined for transects at cruising speed in all surveys in 1994 and 1995.

Lakes Chao and Tai (China), October 1993. A 15-km-long survey was made in northwestern Lake Chao (31°30′ N, 117°30′ E; A = 760 km^2; Z = 2.6 m). On Lake Tai (31°20′ N, 120°10′ E; A = 2350 km^2; Z = 2 m), seven stations represented a 32-km-long transect from the central basin into Wuxi Bay. Two other stations were located near the mouth of River Lu and the eastern shore in this bay. During extensive wind resuspension, measurements were repeated at the latter site.

Vecht Lakes, May 1994, and Overijssel Lakes (The Netherlands), August 1995. The Vecht (52°10′ N, 5°0′ E) and Overijssel lakes (52°40′ N, 6°0′ E) originated by peat excavation. Surface area ranged from 0.3 to 10 km^2 and in general Z was <2.5 m. The Vecht lakes were Hollands Ankeveen, Stichts Ankeveen, Wijde Gat, Hilversums Kanaal, Loenderveen, Vuntus, Loosdrecht, Breukeleveen, and the up to 30-m deep Spiegelplas, Wijde Blik, and Reservoir of Amsterdam. Additional observations were made on Lake Loosdrecht in August 1994 and November 1996 and on the reservoir in September 1994. The Overijssel lakes were Beulakerwijde, Giethoorn, Duinigermeer, Schutsloterwijde, and Eastern and Western Belterwijde.

Other Lakes (The Netherlands). The large and shallow Lake Markermeer (52°30′ N, 5°20′ E; A = 610 km^2; Z = 3.3 m), the small and relatively deep Lake Vechten (52°4′ N, 5°10′ E; A = 5 ha; Z = 6 m), and the shallow, former sea inlet Lake Lauwersmeer (53°20′ N, 6°10′ E; A = 20 km^2; Z = 2.3 m) were visited in August 1994, June 1995, and June 1997, respectively.

Scheldt Estuary (Belgium−The Netherlands), August 1996. A 60-km-long transect included near-seawater at Terneuzen (51°22′ N, 3°53′ E) and freshwater at central Antwerp.

* Corresponding author fax: +31 294 232224; e-mail: gons@cl.nioo.knaw.nl.

10.1021/es9809657 CCC: $18.00
Published on Web 02/12/1999

TABLE 1. Measurement Conditions, Parameters for the Optical Teledetection of Chlorophyll *a*, Concentrations of Chlorophyll *a* Corrected for Pheopigment (Chl-*a*; mg m^{-3}) and Total Suspended Matter (TSM; g m^{-3}) in Near-Surface Samples, and Secchi-Disk Depth (Z_{SD}; m)[a]

location	*N*	θ_0	μ_{ad}	*Q*	S_{wa}	R	b_b	Chl-*a*	TSM	Z_{SD}
IJssel Lagoon stations										
R. IJssel	12	33−62	0.65−0.80	3.0−3.7	0.09−0.55	0.8−1.2	0.05−1.6	4−33	15−39	0.6−1.0
L. Ketelmeer	12	31−56	0.67−0.83	2.9−3.6	0.09−0.48	0.9−1.6	0.04−1.3	7−44	12−40	0.5−1.0
L. IJsselmeer Urk	12	30−53	0.66−0.83	2.9−3.6	0.06−0.47	0.9−2.6	0.07−1.7	5−85	5−39	0.5−2.5
L. IJsselmeer Medemblik	12	40−60	0.59−0.75	3.2−4.0	0.08−0.50	1.1−2.3*	0.12−1.9*	26−185	8−99	0.3−1.1
IJsselmeer Stavoren	12	52−68	0.60−0.73	3.3−4.0	0.13−0.47	1.1−2.3	0.20−5.2	44−144	14−72	0.4−1.1
IJssel Lagoon transects										
R. IJssel−L. Ketelmeer	6	31−58	0.66−0.77	3.1−3.6	0.10−0.48	0.9−1.3	0.24−2.9	3−34	12−35	
L. Ketelmeer−Urk	12	30−54	0.67−0.84	2.9−3.5	0.15−0.57	0.8−1.5	0.12−1.5	6−33	6−36	
Urk−Medemblik	26	32−55	0.64−0.82	2.7−3.9	0.13−0.51	0.8−3.1	0.07−8.2	7−163	4−94	
Medemblik−Stavoren	11	44−65	0.55−0.73	3.3−4.1	0.12−0.44	1.3−2.8	0.17−1.2	42−106	12−36	
Lake Chao	10	37−39	0.74−0.77	3.1−3.2	0.04−0.12	1.4−4.5	1.01−5.8**	20−994	12−298	
Lake Tai	10	38−50	0.66−0.77	3.1−3.6	0.05−0.28	0.9−1.4	0.23−1.5	5−32	10−36	0.4−1.0
Vecht Lakes	13***	35−78	0.73−0.77	3.1−3.3	0.23−0.88	0.7−3.6	0.01−0.5	2−119	1−28	0.5−4.2
Overijssel Lakes	6	39−78	0.55−0.76	3.1−4.3	0.17−0.61	1.8−2.5	0.07−0.5	8−89	4−31	0.4−1.1
other lakes	3	31−48	0.70−0.84	2.8−3.4	0.11−0.83	0.9−1.5	0.01−0.3	8−52	3−51	0.4−2.8
Scheldt Estuary	9	41−64	0.52−0.75	3.2−4.6	0.08−0.17	0.8−1.8	0.12−1.2	3−93	7−78	0.3−1.8

[a] Symbols: *N*, number of observations; θ_0, sun zenith angle (deg); μ_{ad}, average cosine of downwelling light above water; *Q*, subsurface upward radiance to irradiance conversion factor at specified geometry; S_{wa}, fraction of reflected sky radiance in water-leaving radiance computed for still water (400−700 nm); R, subsurface irradiance reflectance ratio $R(0,704):R(0,672)$; b_b, backscattering coefficient derived from the reflectance at 776 nm (m^{-1}) (*excluding March 1994; **excluding 7 stations; ***including 2 additional observations on Lake Loosdrecht).

Determination of $R(0,\lambda)$

Theory for Still Water. The look direction of a hand-held instrument must have an angle to the vertical in order to avoid shade and reflection from the platform. Measuring in a plane at right angle to the vertical plane of the sun, i.e., at azimuthal angle $\phi = 90°$ or 270°, avoids sun glint as well. Thus, water-leaving radiance L_{wa} involves only refracted upward radiance L_u at nadir angle θ_w in water and reflected sky radiance L_s. Reflectance of the air−water interface is small for angles of incidence < 50°. Because L_u is nearly constant in the 0−30° nadir angle interval (*7*, *21*), i.e., at angles ≤42° for the emergent light, an angle of observation $\theta_a = 42°$ is optimal.

By definition, $R(0,\lambda)$ is the quotient of the spectral upward and downward irradiances immediately below the surface. Upward irradiance $E_u(0,\lambda)$ is approximated by

$$E_u(0,\lambda) = Q(\theta_w,\phi)L_u(\theta_w,\phi,\lambda) = Q(\theta_w,\phi)\{L_{wa}(\theta_a,\phi,\lambda) - \rho(\theta_a)L_s(\theta_a,\phi,\lambda)\}\{1 - \rho(\theta_w)\}^{-1}n^2 \quad (1)$$

where $Q(\theta_w,\phi)$ is a geometrical factor; $\rho(\theta_a)$ and $\rho(\theta_w)$ are Fresnel reflectance for L_s and L_u, respectively; and n is the relative refraction index of water. For freshwater, $n = 1.333$, $\rho(\theta_w = 30°) = 0.0214$, and $\rho(\theta_a = 42°) = 0.0256$. For turbid water, Q is expected to be around 3.5 (*6*, *21*).

Downward irradiance $E_d(0,\lambda)$ consists of the refracted solar beam and diffuse sky light and a downward reflected part of upwelling light that equals $0.5E_u(0,\lambda)$ (*7*). $E_d(0,\lambda)$ is obtained from downward irradiance above water $E_{ad}(\lambda)$ according to

$$E_d(0,\lambda) = E_{ad}(\lambda)\{1 - \rho(\theta_0)(1 - F(\lambda)) - r_dF(\lambda)\} + 0.5E_u(0,\lambda) \quad (2)$$

where $F(\lambda)$ is the fraction of diffuse light in $E_{ad}(\lambda)$, and $\rho(\theta_0)$ and r_d are Fresnel reflectance for solar beam at zenith angle θ_0 and average reflectance for diffuse light, respectively. For r_d, a value of 0.06 (*7*) is reasonable for general application.

Surface Wave Effect. Waves impose fluctuations in the contribution of L_s. An instrument as used here records $L_{wa}(\theta_a = 42°, \varphi = 90°)$ from a plane element of water surface of 0.1−0.2 m in diameter. The slope oscillates depending on the wave characteristics. Wave height and period (T) depend on wind speed (U), fetch (l), and water depth (Z), and wavelength depends on T and Z. For $U = 5$ m s^{-1} (gentle breeze) up to 20 m s^{-1} (gale), shallow lakes exhibit waves as steep as 9−15°, with T ranging from 1 to 4.5 s (*22*). For a small ($l = 1$ km, $Z = 1.5$ m) and a large lake ($l = 25$ km, $Z = 4.5$ m), potential contribution of L_s for $U = 5$−20 m s^{-1} was examined as a percentage of the contribution for still water. Computations were made for progressive sinusoidal waves (*22*) under isotropic radiance representing clear sky and standard overcast sky (*7*). The contribution of L_s did not vary greatly depending on wind and lake dimension. Greatest fluctuations from 82 to 194% were simulated for coinciding directions of view and wave propagation under a clear sky. Wave-period averaged contributions varied from 102% for $U = 5$ m s^{-1} under overcast sky to 119% for $U = 20$ m s^{-1} under clear sky. Thus, error in $R(0,\lambda)$ might be large if the scan time (ST) of L_{wa} is short as compared to T but is acceptable for ST = T or a multiple thereof. For photosynthetically available radiation (PAR; 400−700 nm) the error can be evaluated from fraction S_{wa} of reflected L_s in L_{wa} (Table 1). In general, S_{wa} varied from about 0.1 under sunlight to 0.5 under overcast sky.

Instrumentation and Application. A model PR-650 SpectraColorimeter (Photo Research, Chatsworth, CA), featuring 1°-measuring optics and a 128-element diode array, acquired spectra from 380 to 780 nm. Full-width half-maximum bandwidth was 8 nm. Selection of integration time (IT) and correction for dark signal of the same IT were automatic. Scan time of one spectrum was thus >2IT. An ICM card had a storage capacity of 580 spectra. The instrument was held about 4 m above water on the lagoon and estuary and between 1.5 and 2.5 m elsewhere. The averages of 10 spectra were recorded for $L_{wa}(\theta_a,\phi,\lambda)$ and $L_s(\theta_a,\phi,\lambda)$ (eq 1) and the radiances from a sunlight-exposed and next shaded reference plaque to determine $E_{ad}(\lambda)$ and $F(\lambda)$ (eq 2).

For two surveys on the lagoon in the rain, $L_s(\theta_a,\phi,\lambda)$ was computed from the reference radiance assuming standard overcast sky. IT for L_{wa} on the lagoon was ≥100 ms, making ST > 2 s. Short IT generally coincided with small S_{wa}. For very big waves in March 1994, IT was ≥550 ms. The setting of 10 spectra to average also provided reasonably long scans elsewhere.

Subsurface Spectral Reflectance in Situ. To test the determination of $R(0,\lambda)$ (eqs 1 and 2), a comparison was made with $R(0,\lambda)_w$ from $E_u(0,\lambda)$ and $E_d(0,\lambda)$ in situ. Study sites were highly turbid Lake Loosdrecht in August and the clear Reservoir of Amsterdam in September 1994. The water surface was flat under somewhat hazy sky and slightly rippled under overcast sky, respectively. For stable light and still water and $R(0,\lambda)$ computed assuming $Q(\theta_w,\phi) = \pi$, the true value of Q is close to $R(0,\lambda)_w/\{\pi R(0,\lambda)\}$. For measurement in water, the PR-650 lens was replaced with a 4-m-long quartz light guide from a cosine collector (Macam, Livingston, U.K.) in a housing of 3.5 cm o.d. Sensor self-shading lowers $E_u(0,\lambda)$ in proportion to total absorption $a(\lambda)$ and radius (r) of the sensor housing (*23*). The total absorption, calculated from optical densities of filtrates and of particles on filters (*24*) and absorption by water (*25*), varied from 1.4 to 10.6 m^{-1} in the lake and from 0.5 to 4.1 m^{-1} in the reservoir.

For the lake, $R(0,\lambda)$ was lowest in the violet waveband and exhibited major peaks at 584 and 704 nm, i.e., typical for shallow Vecht and Overijssel lakes (Figure 3). Standard error (se) at 584 nm was 1.7% ($N = 3$). Two $R(0,\lambda)_w$ spectra differed 1% at 584 nm but by a factor of 3 in the violet band. The light guide imposed maximal IT (6 s) for $E_u(0,\lambda)$ and, therefore, inaccuracy for bands with very low upwelling light. Average $R(0,\lambda)_w$ was lower than $R(0,\lambda)$, i.e., 5% at 584 nm up to 20% in violet and near-infrared (NIR). Sensor-shading factor $a(\lambda)r$ was 0.03 for 584 nm, in theory (*23*) giving an error of 5−10%. Predicted errors for 380 and 750 nm were around 50 and 15%, respectively. While the comparison was inaccurate for 380 nm, sensor shading largely explained difference between $R(0,\lambda)_w$ and $R(0,\lambda)$ from the blue band up to NIR. Therefore Q was close to π.

The reservoir showed low $R(0,\lambda)$ at all wavelengths, cf. the lowest spectrum in Figure 3. The shading effect was small, but also here $E_u(0,\lambda)$ required maximal IT. $R(0,\lambda)$ and $R(0,\lambda)_w$ were not significantly different between the violet and NIR bands. Again, Q was close to π.

Incident Light and Surface Roughness. Dependence of Q on sun angle and sky condition and adjustment of $\rho(\theta_a) = 0.0256$ for general application were calibrated to $R(0,PAR)_w$ in situ. Average cosines μ_{ad} (Table 1) and $\mu(0)$ for downwelling light above and refracted light immediately below the surface, respectively, were computed from θ_0 and F(PAR). Sky radiance was assumed to be isotropic for clear skies and variable cloud cover and to be cardioidal for overcast skies. Sensor shading was insignificant for PAR as measured by using quantum sensors from Li-Cor (Lincoln, NE). $R(0,PAR)_w$ was calculated from $E_u(z,PAR)$ and $E_d(z,PAR)$ for $z \leq 0.1z_m$, where z_m is the depth at which $E_d(z,PAR) = 0.1E_d(0,PAR)$ (*7*). This restriction excluded 18 observations with big waves. Considering Q and μ inversely related (*6, 21*), $Q(\theta_w,\phi)$ (eqs 1 and 2) was substituted by $m/\mu + n$, where m and n are parameters to fit. Regression of $R(0,PAR)_w$ to $R(0,PAR)$ with $\rho(\theta_a) = 0.0256$ was slightly better with $\mu = \mu_{ad}$ than $\mu = \mu(0)$, and weight n proved insignificant. Regression for $Q = m/\mu_{ad}$ gave $m = 2.28 \pm 0.06$ ($R^2 > 0.89$; $N = 42$). Results for $Q = m/\mu_{ad}$ and parameter to fit ρ^* substituting $\rho(\theta_a)$ were $m = 2.38 \pm 0.07$, and $\rho^* = 0.0293 \pm 0.0013$ ($R^2 = 0.91$; Figure 1).

In theory, Q may range from 0.3 to 6.5 (*21*) but is expected to be 3−4 for $\theta_w < 35°$ in turbid water (*6, 21*), as empirically derived for river water (*4*). Values of $Q = 2.38/\mu_{ad}$ ranged from 2.7 to 4.6 for high vs low sun (Table 1) and were consistent with the observations on $R(0,\lambda)$ in situ. Predictions for the lake and reservoir were 3.2 and 3.3. Increase from the still water value $\rho(\theta_a) = 0.0256$ to $\rho^* = 0.029$ seemed realistic regarding effects of waves and foam.

Spectra of Turbid Inland Waters. Diversity of water (Table 1) was manifested by the $R(0,\lambda)$ spectra (Figures 2 and 3; all for $Q = 2.38/\mu_{ad}$ and $\rho^* = 0.029$), which may be compared with those for various water as obtained in situ (*26*). All spectra showed valleys from 668 to 680 nm, i.e., around red absorption peaks of Chl-*a* in vivo. Accessory pigments were indicated by local minima from 604 to 636 nm. Contrary to clear water (*7, 26*), $R(0,\lambda)$ could be determined up to 780 nm. At high [Chl-*a*] the peaks occurred at $\lambda > 700$ nm, as explained by opposite change in absorption by pigment and water for nearly constant backscattering.

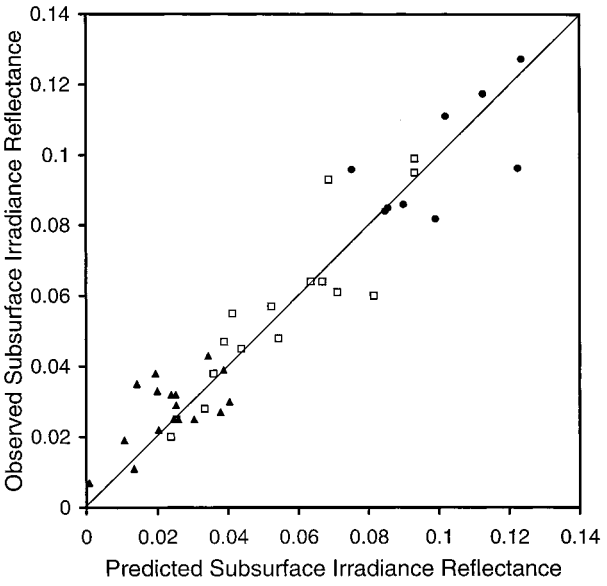

FIGURE 1. Subsurface irradiance reflectance of photosynthetically available radiation (PAR) obtained from upward and downward quantum irradiance of PAR measured in situ vs the values computed from measurements (eqs 1 and 2) for $Q(\theta_w,\phi) = 2.38/\mu_{ad}$ and $\rho^* = 0.029$, see text (solid circles: Lake Tai; squares: IJssel Lagoon; solid triangles: Vecht and Overijssel lakes).

The lagoon embodied transformations of silt-laden river water to highly eutrophic lake water. Lowest $R(0,\lambda)$ occurred for relatively clear water in the transition zone in southern Lake IJsselmeer. Values were >0.15 for extensive sediment resuspension and approached the limit of 0.275 (*31*) for [TSM] up to 99 g m^{-3} during Beaufort-8 wind. Absorption by inanimate particles at 440 nm was up to 7 m^{-1} in March 1994, i.e., nearly three times the high records for DOM and phytoplankton.

In Lake Chao compact, green floating layers alternated with <1-cm-wide, yellowish streaks of *Microcystis* sp. $R(0,\lambda) > 0.3$ was computed for NIR. Marked valleys around 440 nm signified the Chl-*a* Soret band, which was masked by DOM and particles in well-mixed water bodies. The compact layers were distinguished by the $R(0,\lambda)$ ratio for 780 and 700 nm, which together with the ratio for 440 and 380 nm also set apart the streaks from the other study sites.

The families of curves for Lake Tai and the estuary expressed an increase in [Chl-*a*] and [TSM] from the central basin to River Lu and from the mouth upstream into the maximum turbidity zone, respectively. Highest $R(0,\lambda)$ for Lake Tai signified [TSM] doubling by sediment resuspension from a near gale. In most other lakes, $R(0,\lambda)$ was comparatively low, withstanding [TSM] up to 31 g m^{-3}. In Overijssel lakes, DOM absorption at 440 nm was >6 m^{-1} at dissolved organic carbon concentrations >30 g m^{-3}. Three spectra indicated that the surface roughness correction was too large for wavelets under very low sun. In Lake Duinigermeer dense benthic growth of *Characeae* was visible. This case stood out by low $R(0,\lambda)$ with the peak at 704 nm and a valley centered at 608 nm. Compared to the other sites, relatively deep lakes exhibited very low $R(0,\lambda)$ for $\lambda > 550$ nm.

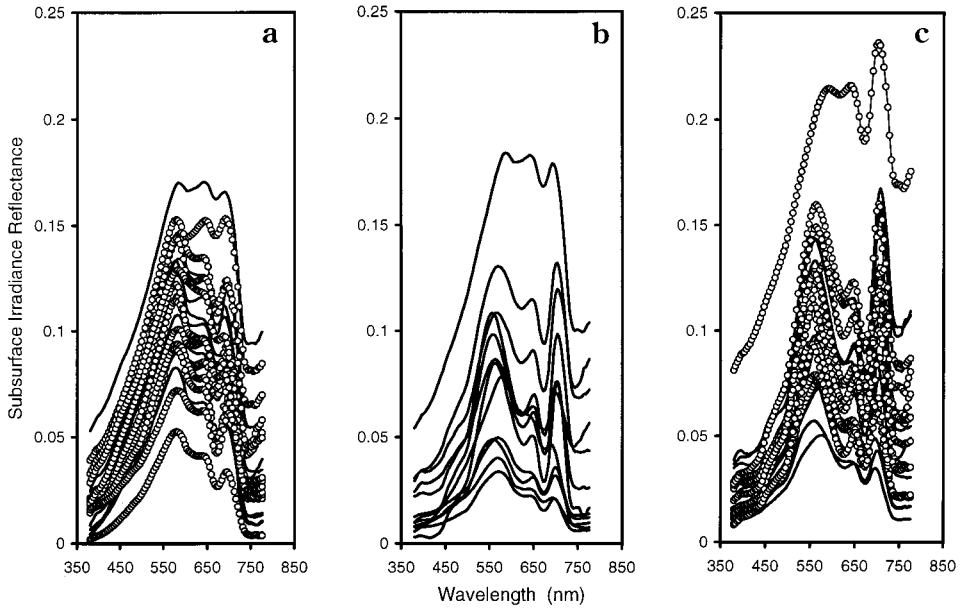

FIGURE 2. Subsurface spectral irradiance reflectance determined for the IJssel Lagoon stations during 1993−1996. a: River IJssel (solid lines) and Lake Ketelmeer (circles); b: Lake IJsselmeer near Urk (solid lines); c: Lake IJsselmeer near Medemblik (solid lines) and Stavoren (circles).

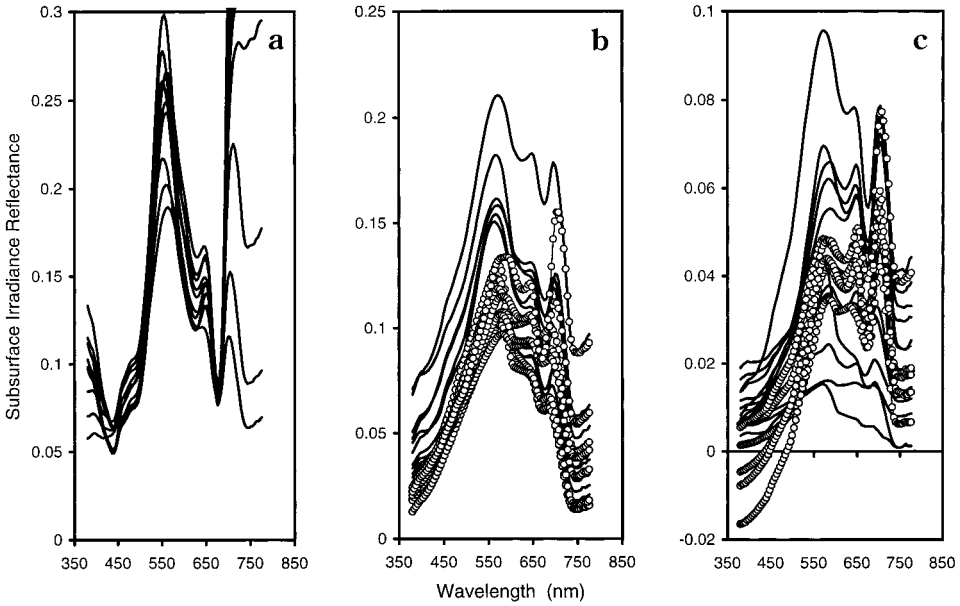

FIGURE 3. Subsurface spectral irradiance reflectance determined for Lake Chao (a, solid lines), Lake Tai (b, solid lines) and Scheldt Estuary (b, circles), and Dutch lakes (c, Overijssel lakes: circles; other lakes: solid lines). Additional spectra of Lake Loosdrecht and Reservoir of Amsterdam not shown.

Retrieval of [Chl-*a*] from $R(0,\lambda)$

Algorithm Development. Ratio of reflectance near 705 nm to that near 675 nm proved useful for retrieval of [Chl-*a*] in eutrophic water (*9, 10, 12, 14, 27*). The feature of turbid water that $R(0,\lambda)$ can be determined for NIR was used to also involve the coefficients of absorption $a(\lambda)$ and backscattering $b_b(\lambda)$ according to the approximation (*28−30*)

$$R(0,\lambda) = Cb_b(\lambda)/\{a(\lambda) + b_b(\lambda)\} \quad (3)$$

where the scaling factor C depends on incident light in a similar manner as Q (*21*). From eq 3, reflectance ratio R for $\lambda = 704$ and 672 nm can be written as

$$R = \{a(672) + b_b(672)\}/\{a(704) + b_b(704)\} \quad (4)$$

Absorption can be partitioned among phytoplankton (a_{ph}), water (a_w), DOM (a_h), and inanimate particles (a_d) (*7, 17*). The simplifications are made that (i) for $\lambda = 672$ nm, absorption other than by Chl-*a* and water is negligible; (ii) for $\lambda = 704$ nm, a_{ph}, a_h, and a_d are insignificant in comparison to a_w; and (iii) b_b is wavelength independent. Thus $a_{ph}(672)$ equals $a_{Chl}(672)$, the product of [Chl-*a*] and Chl-*a*-specific coefficient $a^*(672)$. By rearrangement of eq 4, [Chl-*a*] and R are equated:

$$[\text{Chl-}a] = \{R(a_w(704) + b_b) - a_w(672) - b_b\}/a^*(672) \quad (5)$$

Values of b_b can be derived from $R(0,\lambda)$ in NIR where absorption by other substances is very small as compared to a_w (*7*). Equation 3 proved accurate for experiments under diffuse light, in which C did not differ significantly from

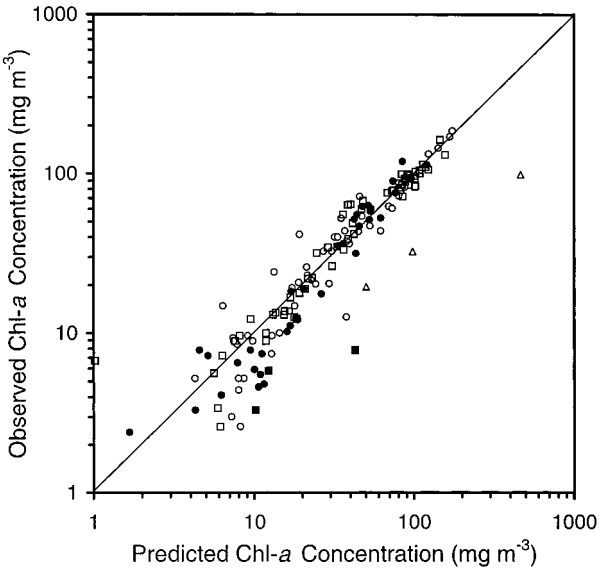

FIGURE 4. Concentrations of chlorophyll *a* in near-surface samples vs the values computed from subsurface spectral irradiance reflectance (eq 6) for IJssel Lagoon stations ($N = 59$; circles) and transects ($N = 55$; squares), optically deep water elsewhere, including two additional observations on Lake Loosdrecht ($N = 37$; solid circles), optically shallow sites including Lake Duinigermeer ($N = 4$; solid squares), and Lake Chao stations exhibiting surface streaks of *Microcystis* sp. ($N = 3$; triangles).

asymptote $R(0,\lambda) = 0.275$ (*30*). Applying $Q = 2.38/\mu_{ad}$ for isotropic radiance ($\mu_{ad} = 0.703$), the ratio C/Q was 0.082, i.e., close to a similar ratio for oceanic water (*21*). Equation 3 with $C = 0.082Q$ was used for deriving b_b at $\lambda = 776$ nm. This wavelength is optimal regarding absorption by water relative to photosynthetic pigments and detritus, absorption by atmospheric O_2 near 760 nm, and temperature sensitivity (*25*). Values of b_b (Table 1) varied from 0.012 m^{-1} in the reservoir to 8.2 m^{-1} in Lake IJsselmeer in March 1994.

Calibration. The lagoon data for stations (Table 1; Figure 2) suited model testing because the platform of observation had been identical throughout the study and the potential effect of a vertical gradient was known. Regression of [Chl-*a*] in near-surface vs depth-integrated samples gave a slope of 1.00 ± 0.04 and an intercept of 1.2 ± 2.5 mg m^{-3} ($R^2 = 0.92$; $N = 60$). However, considerable [Chl-*a*] difference, even up to 68 mg m^{-3}, was recurrent at the station Urk.

Regression of eq 5 gave $a^*(672) = 0.0178 \pm 0.0004$ m^2 (mg of Chl-*a*)$^{-1}$ ($R^2 > 0.94$; $N = 59$). Greatest residual was 48 mg m^{-3} for March 1994 with $b_b = 5.2$ m^{-1}. The model significantly improved ($R^2 > 0.96$) by assigning a power to the second backscattering coefficient in eq 5:

$$[\text{Chl-}a] = \{R(a_w(704) + b_b) - a_w(672) - b_b{}^p\}/a^*(672) \quad (6)$$

Values of $a^*(672)$ and exponent p were 0.0175 ± 0.0003 and 1.09 ± 0.01, respectively. Greatest residual was 26 mg m^{-3} for incomplete mixing at station Urk in September 1993. Due to rain, $R(0,\lambda)$ might have been inaccurate for all stations in 1993. Their exclusion did not result in a change of $a^*(672)$ and p.

Calibration of eq 6 for stations and transects resulted to $a^*(672) = 0.0176 \pm 0.0002$ and $p = 1.065 \pm 0.007$ ($R^2 > 0.95$; $N = 114$) and showed no systematic difference between the data groups (Figure 4). Prediction for March 1994 was highly sensitive to the exponent. Two negative [Chl-*a*] values would have resulted from $p = 1.09$. Concentrations with apparent negative pheopigment content ($N = 13$) were underpredicted, but their exclusion did not affect $a^*(672)$ and p. For all variability, including vertical gradient, se of estimate was 8.9 mg m^{-3} ($N = 114$). For uncorrected Chl-*a* ([Chl-*a*-u] = [Chl-*a*] + [pheopigment]/1.7) the parameters were $a^*(672) = 0.0152 \pm 0.0002$ and $p = 1.056 \pm 0.006$ ($R^2 > 0.96$; $N = 114$).

Validation. The algorithm for Chl-*a* (eq 6) with $a^*(672)$ and p as calibrated for the lagoon proved to be adequate elsewhere (Figure 4). Greatest residual for well-mixed, optically deep lakes in The Netherlands was 15 mg m^{-3}, which was 17% of [Chl-*a*] in Lake Giethoorn. For Lake Loosdrecht with still water ([Chl-*a*] = 119 mg m^{-3}), the concentration was underpredicted by 34 mg m^{-3}, but for the well-mixed lake in May (60 mg m^{-3}) and November (113 mg m^{-3}), residuals were ≤8 mg m^{-3}. Residuals for Lake Tai and the estuary were ≤12 and ≤7 mg m^{-3}, respectively. For extensive resuspension in Lake Tai, the residual was 2 mg m^{-3}.

In three lakes, the bottom was not visible but possibly enhanced $R(0,\lambda)$ at 704 nm and thus predicted [Chl-*a*]. This effect appeared to be significant, but the deviation was not large. Benthic growth as in Lake Duinigermeer may increase $R(0,\lambda)$ at 704 nm while lowering it at 672 nm. In this case, [Chl-*a*] was overpredicted by a factor of 6. For compact floating layers in Lake Chao, negative values of b_b were computed. For the surface streaks, [Chl-*a*] was greatly overpredicted.

Validation of the algorithm for Chl-*a* except for Lakes Chao and Duinigermeer gave an se of estimate = 8.5 mg m^{-3} ($N = 40$). Validation for Chl-*a*-u gave similar results.

Discussion

Modeling Aspects. Gordon et al. (*28*, *29*) fitted ratios of $R(0,\lambda)$ to Q from Monte Carlo simulations to a polynomial expansion of $b_b(\lambda)/\{a(\lambda)+b_b(\lambda)\}$. Values of $b_b(776)$ solved by using this model (*29*) from $R(0,776)$, Q and $a(776) = a_w(776)$ were on average one-third lower than by using eq 3 with $C/Q = 0.082$. Similar discordance resulted by applying $R(0,776) = fb_b(776)/a_w(776)$ for $f/Q = 0.09$ (*21*), and a relationship for highly turbid water (*2*) yielded still lower b_b. For the reservoir, b_b was close to 0.012 m^{-1} in all models, but for the lagoon the greatest value varied from 1.4 m^{-1} (eq 2) to 8.2 m^{-1} (eq 3). Because the suspensions of polystyrene microspheres used to test eq 3 (*30*) embodied the same phase function as the Monte Carlo studies, the divergence of the model results for relatively clear vs highly turbid waters appears to be fundamental. Regarding the widely different backscattering ratios among phytoplankton and other particles (*7*, *17*, *32*, *33*), a single phase function is not likely to represent all situations. Particle sizes may drastically increase by resuspension of sediment, and the exponent p (eq 6) may signify correction of eq 3 for this effect. Resuspension may also limit the validity of small NIR absorption by particles relative to water. Another possibility is increase in apparent b_b by the trapping of air into turbulent water as the lagoon in March 1994.

The $a^*(672)$ coefficient is known to depend on cell size and aggregation and on intracellular concentration and compartmentation of the pigment (*7*, *34*). Most study sites exhibited miscellaneous phytoplankton. Diatoms and flagellates dominated in River IJssel, while green algae and cyanobacteria were most abundant in Lake IJsselmeer. Cyanobacteria occurred as <1-μm single cells, small aggregates, filaments of various length and diameter, and visible colonies and flakes. The calibrated values of 0.018 m^2 (mg of Chl-*a*)$^{-1}$ and 0.015 m^2 (mg of Chl-*a*-u)$^{-1}$ are intermediate in ranges for cultures and natural phytoplankton (*34*). Almost all [Chl-*a*] residuals in this work can be explained by variation of $a^*(672)$ between the proximate boundaries of 0.006 and 0.023 m^2 (mg of Chl-*a*)$^{-1}$.

Stochastic Factors. Replicate measurements with fully developed waves and prevalence of cloudless sky resulted in nearly identical $R(0,\lambda)$ spectra. Occasional observation indicated how $R(0,\lambda)$ may change depending on cloud cover

and presence of foam and in turn influence the prediction of [Chl-*a*]. Significant spread is expected for overcast sky because of uneven cloud density and increased S_{wa}. Nevertheless, [Chl-*a*] was adequately predicted even when in rain L_s could not be measured. Under broken cloud, both L_s and E_{ad} may not be properly defined for L_{wa}, and the angular distribution of E_{ad} and contribution of sun glint are unpredictable. On Lake Ketelmeer (June 1995) under chasing white clouds, two $R(0,\lambda)$ spectra were obtained in sunlight, whereas for a third one L_{wa} was measured in sunlight but E_{ad} was largely under cloud. The third spectrum was greatly enhanced between 450 and 720 nm but very low near 380 and 780 nm. Although derived b_b varied from 0.03 to 0.1 m^{-1}, predicted [Chl-*a*] was between 17 and 19 mg m^{-3}.

On the transect Urk−Medemblik (September 1995), navigation obliquely traversed Langmuir streaks (*35*), exhibiting widths >1 m and distances of about 10 m from one another. Two spectra were obtained for between areas and one for long exposure to foam. The latter was 2−3 times as high and flattened as compared to the other spectra and gave b_b as high as 4.0 m^{-1}. Predicted [Chl-*a*] was 91 and 99 mg m^{-3} for minimal and 75 mg m^{-3} for long exposure to foam.

These observations indicated that the algorithm is quite insensitive to noise in $R(0,\lambda)$. Reasons for stable [Chl-*a*] prediction under fluctuating light are the spectral ratioing and near-constancy (eqs 5 and 6) as long as b_b is small as compared to a_w. For high b_b the emergent flux is so strong that S_{wa} tends to be small, thus noise in $R(0,\lambda)$ is alleviated. Despite the b_b increase, the foam effect on predicted [Chl-*a*] was not large because the opacity lowered the ratio R.

Application. $R(0,\lambda)$ was determined for Q from a simplified relationship and for a fixed surface roughness correction. Retrieval of [Chl-*a*], without knowledge a priori of spectral absorption and scattering, was tested for usual 1-day surveys. Use of the $R(0,\lambda)$ ratio for $\lambda = 704$ and 672 nm minimized interference of strong absorption by DOM and inanimate particles. By incorporating b_b estimates from $R(0,\lambda)$ in NIR, the algorithm also corrected for scattering at large variation of detritus, minerals, and phytoplankton. Whereas b_b for the reservoir touched the range for seawater (*21*), the high record for the lagoon was almost 3 orders of magnitude greater. The reservoir delimited water transparency for determination of $R(0,\lambda)$ in NIR.

The method proved operational for [Chl-*a*] from 1 to 185 mg m^{-3}, for [Chl-*a*-u] up to 215 mg m^{-3}, in waters exhibiting DOM absorption at 440 nm from 0.4 to 6.5 m^{-1}, particulate organic matter from 2 to 28 g m^{-3}, and suspended minerals from <1 to 71 g m^{-3}. Spectral signatures of benthic algae and cyanobacterial floating layers were identified. Due to increased turbidity by eutrophication, decline of wetlands, and soil erosion, the method can be used for lakes and major rivers in densely populated catchments up to subalpine regions. The single optical channel in this work necessitated sequential scanning. Dedicated instruments could provide synchronous radiance recording and continuous reading of [Chl-*a*]. Through $R(0,\lambda)$ vertical light attenuation coefficient and [TSM] may be assessed beside [Chl-*a*] (*7*), while the chromaticity of spectra may also serve water management (*16*, *17*, *36*). The data are compatible with remote sensing applications (*7*, *11*, *13*, *17*), so that on-site observation can be combined with spatial overview. Optical teledetection as described here offers 'all-weather' robust data acquisition in near-real time and thereby information gain at operational cost reduction.

Acknowledgments

Work in China was made possible by special grants from the Academia Sinica and the Royal Netherlands Academy of Arts and Sciences. Qiming Cai and Weimin Chen (Nanjing Institute of Geography and Limnology), Arnold Dekker (Institute for Environmental Studies, Amsterdam), and Jacco Kromkamp (NIOO−Centre for Estuarine and Coastal Ecology, Yerseke) are thanked for cooperation. Acknowledgments are due to Thijs de Boer, Yuwei Chen, Jeannine Ebert, and Hans Hoogveld for technical assistance. This is Publication No. 2478 of The Netherlands Institute of Ecology, Centre for Limnology, Nieuwersluis, The Netherlands.

Literature Cited

(1) Galat, D. L.; Verduin, J. P. *J. Plankton Res.* **1989**, *11*, 925.
(2) Jupp, D. L. B.; Kirk, J. T. O.; Harris, G. P. *Aust. J. Mar. Freshwater Res.* **1994**, *45*, 801.
(3) Yakobi, Y. Z.; Gitelson, A.; Mayo, M. *J. Plankton Res.* **1995**, *17*, 2155.
(4) Whitlock, C. H.; Poole, L. R.; Usry, J. W.; Houghton, W. M.; Witte, W. G.; Morris, W. D.; Gurganus, E. A. *Appl. Opt.* **1981**, *20*, 517.
(5) Gordon, H. R.; Morel, A. Y. *Remote assessment of ocean color for interpretation of satellite visible imagery. A review*; Springer: New York, 1983.
(6) Bukata, R. P.; Jerome, J. H.; Bruton, J. E. *Remote Sens. Environ.* **1988**, *25*, 201.
(7) Kirk, J. T. O. *Light and photosynthesis in aquatic ecosystems*, 2nd ed.; Cambridge University Press: Cambridge, 1994.
(8) Bukata, R. P.; Jerome, J. H.; Bruton, J. E.; Jain, S. C.; Zwick, H. H. *Appl. Opt.* **1981**, *20*, 1704.
(9) Mittenzwey, K.-H.; Ullrich, S.; Gitelson, A. A.; Kondratiev, K. Y. *Limnol. Oceanogr.* **1992**, *37*, 147.
(10) Dekker, A. G.; Malthus, T. J.; Seyhan, E. *IEEE Trans. Geosci. Remote Sens.* **1991**, *29*, 89.
(11) Dierberg, F. E.; Carriker, N. E. *Environ. Sci. Technol.* **1994**, *28*, 16.
(12) Schalles J. F.; Gitelson A. A.; Yacobi Y. Z.; Kroenke A. E. *J. Phycol.* **1998**, *34*, 383.
(13) Millie, D. F.; Baker, M. C.; Tucker, C. S.; Vinyard, B. T.; Dionigi, C. P. *J. Phycol.* **1992**, *28*, 281.
(14) Rundquist, D. C.; Han, L.; Schalles, J. F.; Peake, J. S. *Photogramm. Eng. Remote Sens.* **1996**, *62*, 195.
(15) Gitelson, A.; Stark, R.; Dor, I. *Water Environ. Res.* **1997**, *69*, 1263.
(16) Morel, A.; Prieur, L. *Limnol. Oceanogr.* **1977**, *22*, 709.
(17) Bukata, R. P.; Jerome, J. H.; Kondratyev, K. Ya.; Pozdnyakov, D. V. *Optical properties and remote sensing of inland and coastal waters*; CRC Press: Boca Raton, 1995.
(18) Bukata, R. P.; Jerome, J. H.; Kondratyev, K. Ya.; Pozdnyakov, D. V. *J. Great Lakes Res.* **1991**, *17*, 470.
(19) NEN 6520. Netherlands Institute for Standardization: Delft, 1981.
(20) Nusch, E. A. *Arch. Hydrobiol. Beih. Ergeb. Limnol.* **1980**, *14*, 14.
(21) Morel, A.; Gentili, B. *Appl. Opt.* **1993**, *32*, 6864.
(22) CERC. *Shore protection manual. Vol. I*; U.S. Army Engineer Waterways Experiment Station Coastal Engineering Research Center: Vicksburg, MS, 1984.
(23) Gordon, H. R.; Ding, K. *Limnol. Oceanogr.* **1992**, *37*, 491.
(24) Weidemann, A. D.; Cleveland, J. S. *Limnol. Oceanogr.* **1993**, *38*, 1321.
(25) Buiteveld, H.; Hakvoort, J. H. M.; Donze, M. *Ocean Optics XII Proc. Soc. Photoopt. Inst. Eng.* **1994**, *2258*, 174.
(26) Davies-Colley, R. J.; Vant, W. N.; Wilcock, R. J. *Water Resour. Bull.* **1988**, *24*, 11.
(27) Gitelson, A. *Int. J. Remote Sens.* **1992**, *13*, 3367.
(28) Gordon, H. R.; Brown, O. B.; Jacobs, M. M. *Appl. Opt.* **1975**, *14*, 417.
(29) Gordon, H. R.; Brown, O. B.; Evans, R. H.; Brown, J. W.; Smith, R. C.; Baker, K. S.; Clark, D. K. *J. Geophys. Res.* **1988**, *93*, 10909.
(30) Krijgsman, J. Optical remote sensing of water quality parameters. Interpretation of reflectance spectra. Doctoral thesis, Delft University of Technology, 1994.
(31) Bukata, R. P.; Bruton, J. E.; Jerome, J. H. *Appl. Opt.* **1980**, *19*, 1550.
(32) Ahn, Y.-H.; Bricaud, A.; Morel, A. *Deep-Sea Res.* **1992**, *39*, 1835.
(33) Balch, W. M.; Kilpatrick, K. A.; Trees, C. C. *Limnol. Oceanogr.* **1996**, *41*, 1669.
(34) Bricaud, A.; Stramski, D. *Limnol. Oceanogr.* **1990**, *35*, 562.
(35) Faller, A. J. *Limnol. Oceanogr.* **1969**, *14*, 504.
(36) Davies-Colley, R. J.; Vant, W. N.; Smith, D. G. *Colour and clarity of natural waters*; Ellis Horwood: Chichester, 1993.

Received for review September 18, 1998. Revised manuscript received December 22, 1998. Accepted January 5, 1999.

ES9809657